JOURNAL OF MODERN OPTICS, 1994, VOL. 41, NO. 7, 1495–1505

Optimal concentration of electromagnetic radiation

C. J. R. SHEPPARD and K. G. LARKIN
Physical Optics Department, School of Physics,
University of Sydney, New South Wales 2006, Australia

(*Received 11 November 1993 and accepted 8 March 1994*)

Abstract. For complete spherical concentration of light the maximum theoretically possible total energy density for a given power input can be, in principle, achieved by appropriate choice of polarization and angular amplitude variation. Illumination of a focusing system with a plane-polarized wave creates at the focus equal electric and magnetic energy densities. By appropriate choice of radial variation this energy density can be maximized. For hemispherical concentration the electric energy density can be seven sixteenths of the maximum possible for a given power input, and the total energy density can be seven eighths of the maximum possible. Focusing by optical systems satisfying the sine condition amongst others is also considered. For a system satisfying the sine condition, the total energy density can be $\frac{64}{75}$ of the maximum possible.

1. Introduction

Bassett [1] has established an upper bound to the energy density which is attainable by passive concentration at any point O for a given input power. He assumes that the point is many wavelengths from any object and that any radiation which is subsequently reflected or scattered back to the point can be neglected. This is equivalent to assuming a high Fresnel number in a focusing system, that is that the (electromagnetic generalization of the) Debye theory is appropriate.

Richards and Wolf [2] have considered the electric and magnetic energy density in the focal region of a lens satisfying the sine condition in the Debye approximation. It is interesting to consider how close a real focusing system can come to the maximum attainable energy density given by Bassett. Later workers have generalized the method of Richards and Wolf to other illumination distributions, including Gaussian weighting, annular pupils, parabolic mirrors and so on [3–6].

Bassett's method is to expand the field in terms of a multipole expansion. These multipole fields are Green functions, that is they satisfy Maxwell's equations for any point other than the point O. The field at O vanishes for any other than the electric and magnetic dipole components. Bassett's upper bound is the energy density produced from a combination of these dipoles, each oriented in three orthogonal directions. Thus this upper bound can be achieved by illumination with a combination of these dipole fields. Sheppard [6] has shown that the polarization, as given by Richards and Wolf [2], produced when a plane-polarized wave is refracted to produce a spherically convergent wave is the same as that for the sum of an electric and a magnetic dipole whose axes are two orthogonal directions in the

0950–0340/94 $10·00

focal plane. Thus with appropriate weighting the plane-polarized wave can be coupled completely into electric and magnetic dipole fields.

2. Energy density at the focus for mixed-dipole fields

Consider a focusing system in which the monochromatic illumination over the Gaussian reference sphere has a polarization given by Richards and Wolf [2] for focusing of a plane-polarized wave, that is it is the sum of two orthogonal electric and magnetic dipole fields and has an electric field amplitude $E_i(\theta)$ which is axially symmetric. Then, if the radius of the reference sphere is f, and α is the angular semiaperture of the optical system (figure 1) the power flow into the system is

$$S = \pi f^2 \left(\frac{\varepsilon}{\mu}\right)^{1/2} \int_0^\alpha |E_i(\theta)|^2 \sin\theta \, d\theta. \tag{1}$$

The electric field amplitude at the focus O is given by Richards and Wolf [2] as

$$E_0 = \frac{f^2\pi^2}{\lambda^2} \int_0^\alpha E_i(\theta)(1 + \cos\theta) \sin\theta \, d\theta. \tag{2}$$

The electric energy density at focus is

$$\begin{aligned} W_e &= \tfrac{1}{4}\varepsilon_0 E_0^2 \\ &= \tfrac{1}{16} k^2 \varepsilon_0 f^2 \left| \int_0^\alpha E_i(\theta)(1 + \cos\theta) \sin\theta \, d\theta \right|^2. \end{aligned} \tag{3}$$

We introduce the factor F_e (the normalized electric energy density) given by

$$F_e = \frac{W_e}{S} = \frac{k^2}{16\pi c} \left| \int_0^\alpha E_i(\theta)(1 + \cos\theta) \sin\theta \, d\theta \right|^2 \Big/ \int_0^\alpha |E_i(\theta)|^2 \sin\theta \, d\theta. \tag{4}$$

By Schwarz's inequality, F_e is maximized when

$$E_i(\theta) = 1 + \cos\theta, \tag{5}$$

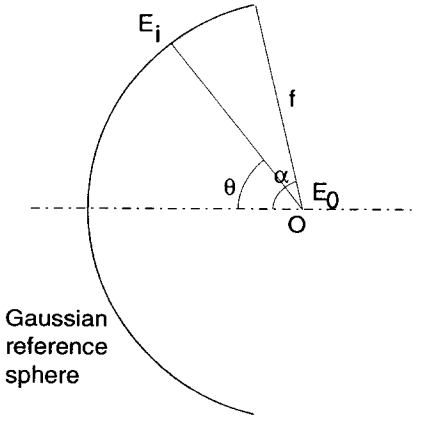

Figure 1. Geometry of concentration.

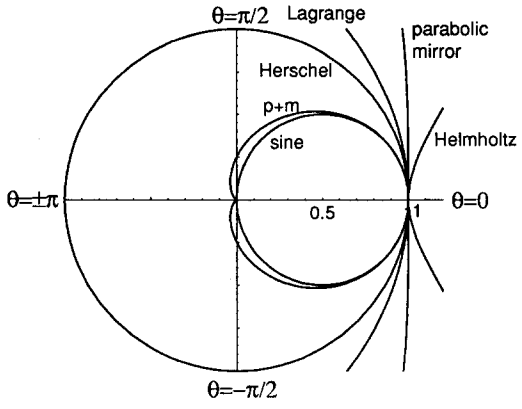

Figure 2. A polar plot of the illumination power incident on the focus O, normalized to unity for $\theta = 0$, for various conditions. In particular, $p + m$ refer to the case of an electric dipole field, oriented along the x axis, and a magnetic dipole field, oriented along the y axis (mixed-dipole field).

and then, when $\alpha = \pi$,

$$F_e = \frac{k^2}{16\pi c}\int_0^{\pi}(1+\cos\theta)^2\sin\theta\,d\theta = \frac{k^2}{6\pi c}. \tag{6}$$

In a similar way we obtain an equal value for F_m, the ratio of the magnetic energy density to the input power, so that the normalized total energy density

$$F = \frac{k^2}{3\pi c}, \tag{7}$$

which is identical with Bassett's upper bound. This particular choice of illumination distribution matches the field of the sum of an electric dipole and an orthogonal magnetic dipole. We therefore shall refer to it as a mixed-dipole wave. It is the electromagnetic analogue of Stamnes' [7] perfect wave. It can also be regarded as the electromagnetic generalization of the Luneberg [8] apodization problem. The illumination power varies as $(1+\cos\theta)^2$, that is it decreases to zero as $\theta \to \pi$. The illumination power, normalized to unity in the forward direction, is shown as a polar plot in figure 2, where it is also compared with other illumination distributions [9]. In particular, for a system satisfying the sine condition, for which

$$E_i(\theta) = \cos^{1/2}\theta, \tag{8}$$

the illumination pattern is quite similar to the mixed-dipole case, so that we expect that the energy density which can be achieved is almost as high. For a mixed-dipole wave, equal electric and magnetic energy densities are excited, so that the electric energy density can only be half that of Bassett's upper bound. The value of F_e for systems of different aperture is shown in figures 3 and 4. For hemispherical illumination the mixed-dipole case can achieve a total energy density of seven eighths of the upper bound, or an electric energy density $F_e = \frac{7}{16}k^2/3\pi c$. The results are summarized in table 1. For an arbitrary system illuminated with a plane wave, the radius r in the pupil plane is related to the angle subtended at O by [8]

$$r = fg(\theta) \tag{9}$$

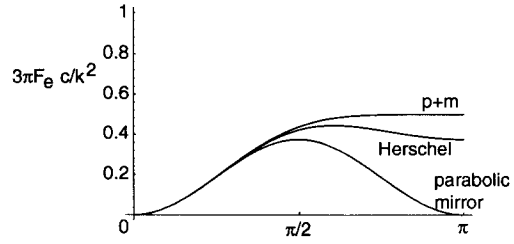

Figure 3. The ratio of the electric energy at the focus to the incident power, as a function of the angular semiaperture α for various different conditions.

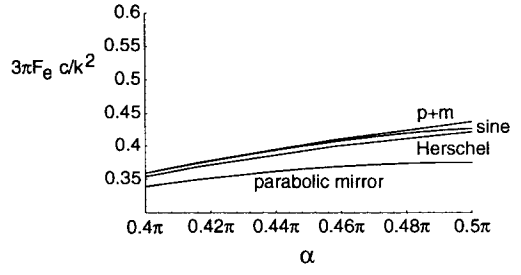

Figure 4. The ratio of the electric energy at the focus to the incident power, as a function of the angular semiaperture α for various different conditions. A system obeying the sine condition behaves very similarly to the mixed-dipole field.

Table 1. F_e and F values for various conditions.

Condition	$F_e(\frac{1}{2}\pi)$	$F(\frac{1}{2}\pi)$
Mixed dipole	0·437	0·875
Sine	0·427	0·853
Herschel	0·422	0·844
Optimum at $\alpha = \arccos\frac{1}{3}$	0·444	0·889
Parabolic mirror	0·375	0·75

and expressions for $g(\theta)$, and the resulting weighting functions $a(\theta)$ given by [10]

$$a(\theta) = \left(\frac{g(\theta)g'(\theta)}{\sin\theta}\right)^{1/2} \tag{10}$$

are given in table 2 after normalizing to unity for $\theta = 0$. As the case of the sine condition gives very similar results to the mixed-dipole case, the former is not shown in figure 3 but instead is illustrated in the expanded plot in figure 4. It should also be noted that all the cases with mixed-dipole polarization exhibit the same behaviour for small values of α. Explicit expressions for $F_e(\alpha)$ are also given in table 2.

3. Energy density in the focal region for a mixed-dipole wave

The mixed-dipole wave produces for hemispherical illumination a normalized total energy density greater than half the maximum possible. This results because

Table 2. $g(\theta)$, $a(\theta)$ and $6\pi cF_e(\theta)/k^2$ values for various conditions.

Condition	$g(\theta)$	$a(\theta)$	$6\pi cF_e(\theta)/k^2$
Mixed dipole	$2\sin(\frac{1}{2}\theta)[1-\frac{1}{2}\sin^2(\frac{1}{2}\theta)]^{1/2}$	$\cos^2(\frac{1}{2}\theta)$	$1-\cos^6(\frac{1}{2}\alpha)$
Sine	$\sin\theta$	$\cos^{1/2}\theta$	$\frac{64}{75}[1-\frac{5}{8}\cos^{3/2}\alpha(1+\frac{3}{5}\cos\alpha)]^2/\sin^2\alpha$
Herschel	$2\sin(\frac{1}{2}\theta)$	1	$3\sin^2(\frac{1}{2}\alpha)[1-\frac{1}{2}\sin^2(\frac{1}{2}\alpha)]^2$
Parabolic mirror	$2\tan(\frac{1}{2}\theta)$	$\sec^2(\frac{1}{2}\theta)$	$\frac{3}{4}\sin^2\alpha$
Lagrange	θ	$\left(\frac{\theta}{\sin\theta}\right)^{1/2}$	
Helmholtz	$\tan\theta$	$\sec^{3/2}\theta$	

the field of the mixed-dipole tends to cancel out in the backward direction. The variation in the polarization of the mixed-dipole wave is shown in figure 5. The wave is almost plane polarized in the forward direction C and exhibits a singularity in polarization in the backward direction A.

The field in the focal region of the mixed-dipole wave can be calculated from the expressions of Richards and Wolf [2]. For the complete mixed-dipole wave ($\alpha \to \pi$) the integrals of Bessel functions for the field in the focal plane can be evaluated using the identity (equation (11.4.10) in [11])

$$\int_0^{\pi/2} J_\mu(z\sin t)\sin^{\mu+1}t\cos^{2\nu+1}t\,\mathrm{d}t = \frac{2^\nu\Gamma(\nu+1)}{z^{\nu+1}}J_{\mu+\nu+1}(z). \tag{11}$$

The field in the focal plane can be expressed in terms of the following integrals:

$$\int_0^{\pi} J_0(z\sin t)\sin t\,\mathrm{d}t = 2j_0(z), \tag{12}$$

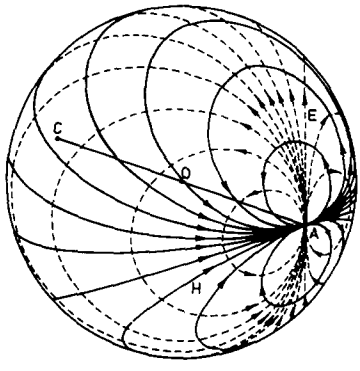

Figure 5. The polarization of the mixed dipole field (after [6]). The point C corresponds to $\theta = 0$ and A to $\theta = \pi$.

$$\int_0^\pi J_0(z\sin t)\sin t\cos^2 t\,\mathrm{d}t = \frac{2}{z}j_1(z) = \tfrac{2}{3}[j_0(z)+j_2(z)], \tag{13}$$

$$\int_0^\pi J_1(z\sin t)\sin^2 t\,\mathrm{d}t = 2j_1(z), \tag{14}$$

$$\int_0^\pi J_2(z\sin t)\sin^3 t\,\mathrm{d}t = 2j_2(z), \tag{15}$$

where j_n is a spherical Bessel function of the first kind and order n.

An alternative approach, which gives the field anywhere in space directly in closed form, is by using the well known expressions for the fields of electric and magnetic dipoles [12]. At any point in space the total field is given by the sum of an outgoing and an incoming wave, giving for an electric dipole oriented along the negative x axis, in cylindrical coordinates ρ, ϕ, z and spherical radius r:

$$\mathbf{E}_\mathrm{p} = \left([j_0(kr)+\tfrac{1}{4}j_2(kr)]\frac{\rho^2}{r^2} + j_2(kr)\frac{3\rho^2}{4r^2}\cos(2\phi) + [j_0(kr)-\tfrac{1}{2}j_2(kr)]\frac{z^2}{4r^2}\right)\mathbf{i}$$

$$+ j_2(kr)\frac{3\rho^2}{4r^2}\sin(2\phi)\,\mathbf{j} + j_2(kr)\frac{3\rho z}{2r^2}\cos\phi\,\mathbf{k}. \tag{16}$$

This expression has been normalized to unity at the origin. Similarly for a magnetic dipole oriented along the y axis,

$$\mathbf{E}_\mathrm{m} = [j_0(kr)+j_2(kr)]\tfrac{1}{2}\mathrm{i}(kz\mathbf{i} - k\rho\cos\phi\mathbf{k})$$

$$= j_1(r)\tfrac{3}{2}\mathrm{i}\left(\frac{z}{r}\mathbf{i} - \frac{\rho\cos\phi}{r}\mathbf{k}\right). \tag{17}$$

Figure 6 shows the electric energy density along the three axes for the electric dipole, the magnetic dipole and the mixed dipole. In each case the variation $\{[\sin(kr)]/kr\}^2$, the intensity for a full spherical scalar wave [13], is shown for comparison. Plots of the electric energy density in the focal plane (figure 7) and in planes containing the axis (figures 8 and 9) are also shown. It is seen that the electric energy density along the x direction actually exhibits a minimum at the origin, so that the maximum electric energy density is slightly greater than half Bassett's upper bound (equal to 0·577 at $kz = 0{\cdot}94$). We can see that the mixed-dipole wave for plane-polarized illumination is thus not suitable for imaging applications. However, for circularly polarized illumination the electric energy density is circularly symmetric and reduces to

$$W_\mathrm{e} = j_0^2(k\rho) + \tfrac{1}{2}j_0(k\rho)j_2(k\rho) + \tfrac{5}{8}j_2^2(kr) + \tfrac{9}{8}j_1^2(kr), \tag{18}$$

which is shown in figure 10.

Along the z axis the field for the plane-polarized case is given by

$$\mathbf{E} = [j_0(kz) - \tfrac{1}{2}j_2(kz) + \tfrac{3}{2}\mathrm{i}j_1(kz)]\mathbf{i} \tag{19}$$

so that the phase is

$$\Phi = \arctan\left(\frac{3j_1(kz)}{2j_0(kz) - j_2(kz)}\right). \tag{20}$$

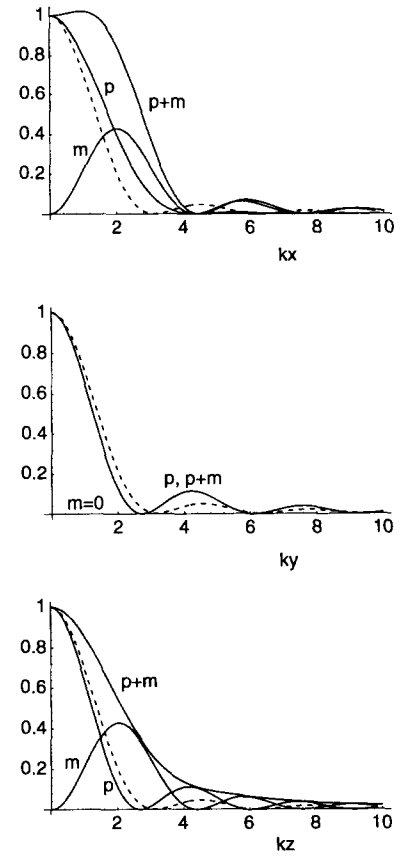

Figure 6. The electric energy density along the x, y and z for an electric dipole field p, a magnetic dipole field m and the mixed-dipole field $p+m$ for $\alpha=\pi$. The function $\{[\sin(kr)]/kr\}^2$ is also plotted (– – –) for comparison.

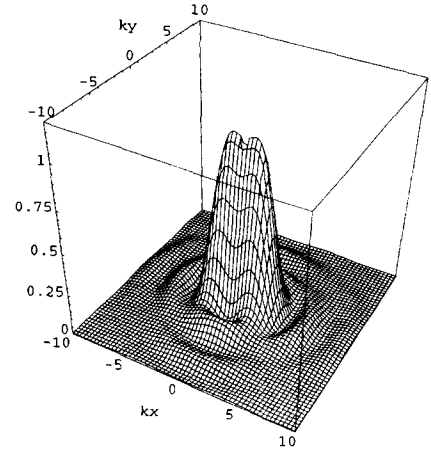

Figure 7. The electric energy density in the focal plane for the mixed-dipole field, $\alpha=\pi$.

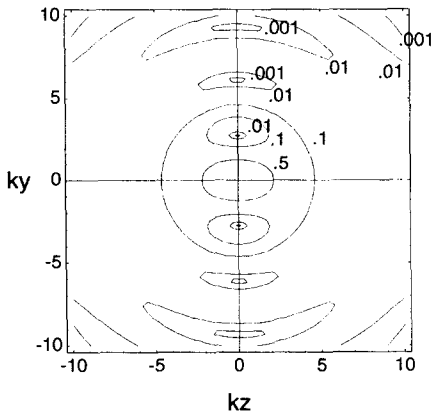

Figure 8. Contour plot N of the electric energy density in the y–z plane for the mixed-dipole field, $\alpha = \pi$.

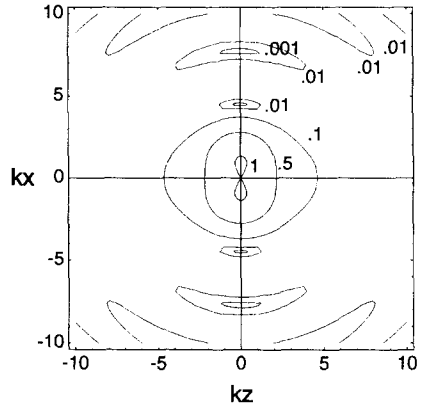

Figure 9. Contour plot N of the electric energy density in the x–y plane for the mixed-dipole field, $\alpha = \pi$.

This is shown in figure 11 with a phase kz suppressed, illustrating the well known phase change of $-\pi$ through focus (the phase anomaly).

4. The hemispherical mixed-dipole wave

If the mixed-dipole wave is truncated, although it matches the field of the mixed dipole exactly within the aperture the truncation results in the generation of multipole terms. For a mixed-dipole wave for $\alpha = \frac{1}{2}\pi$ it is still possible to evaluate the integrals for the field in the focal plane using equation (11). We obtain, after normalizing to unity at the origin,

$$\mathbf{E} = [\tfrac{4}{7}j_0(k\rho) + \tfrac{1}{7}j_2(k\rho) + \frac{6}{7}\frac{J_1(k\rho)}{k\rho} + \tfrac{3}{7}j_2(k\rho)\cos(2\phi)]\mathbf{i}$$

$$+ \tfrac{3}{7}j_2(k\rho)\sin(2\phi)\,\mathbf{j} - \tfrac{6}{7}\mathrm{i}j_1(k\rho) + \frac{J_2(k\rho)}{k\rho}\cos\phi\,\mathbf{k}. \qquad (21)$$

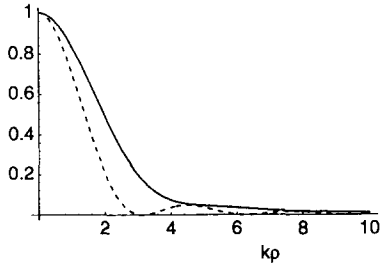

Figure 10. The electric energy density along a radius in the focal plane for circularly polarized illumination, $\alpha = \pi$.

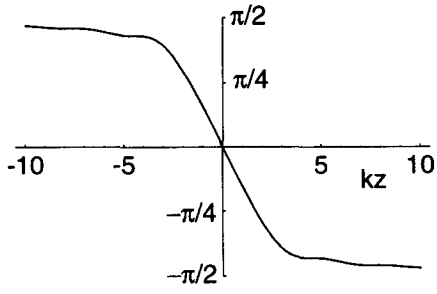

Figure 11. The phase along the axis for the mixed-dipole field, $\alpha = \pi$. A phase kz has been suppressed.

The resulting electric energy density along the x and y axes is illustrated in figure 12. Also shown is the electric energy density for illumination by circular polarization, which is seen to decrease monotonically in the radial direction. An interesting observation is that the electric energy density for plane-polarized illumination exhibits zeros, which is different from the behaviour for a system satisfying the sine condition. The variation in electric energy density in the focal plane for this case is illustrated in figure 13.

5. Discussion

The polarization after focusing which is produced by a focusing system illuminated by a plane-polarized plane wave is identical with that of crossed electric and magnetic multipoles placed at the focus. It can be shown that for a particular form for the angular weighting of the wave incident on the focus a series of multipole terms is excited, and the energy density at focus is maximized by choosing an angular weighting which maximizes the dipole terms. The untruncated mixed-dipole wave produces a total energy density at focus equal to the maximum which is physically possible. If the same angular weighting is truncated, higher-order multipole terms are excited and the energy density at focus is reduced, but the same angular weighting as for the mixed-dipole wave maximizes the focal energy density. Similarly, other forms of angular weighting also result in higher-order multipole terms. A system satisfying the sine condition can achieve $\frac{64}{75}$ of the maximum allowed total energy density. It should prove possible to design optical systems to produce the mixed-dipole weighting, but the improvement over a system satisfying the sine condition is small.

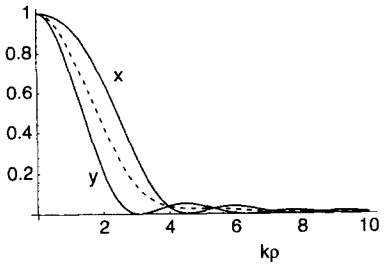

Figure 12. The electric energy density along the x and y axes for the mixed-dipole field, $\alpha = \frac{1}{2}\pi$. The expression $\{[\sin(kr)]/kr\}^2$ is also shown for comparison.

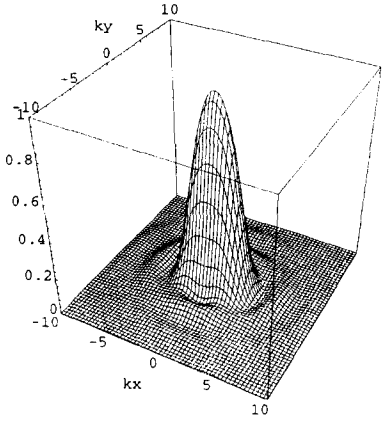

Figure 13. The electric energy density in the focal plane for the mixed-dipole field, $\alpha = \frac{1}{2}\pi$.

It is interesting to note that in scanning imaging systems in which the object is scanned through the focused radiation spot the image is formed by the process of scanning itself, and so there is no necessity for the optical elements to form an image and they only need to concentrate the light to a good focus. Thus the mixed-dipole weighting could give a small improvement in imaging performance of such systems compared with those satisfying the sine condition.

For any arbitrary angular weighting, the energy density in the focal region can be calculated by a multipole expansion rather than by evaluation of the diffraction integrals of Richards and Wolf [2]. This approach has similarities to the method of Kant [14], in which he expands the diffraction integrals in a series of orthogonal polynomials, the terms of which can be associated with terms in the multipole expansion, and will be discussed in a subsequent paper.

Acknowledgments

The authors would like to acknowledge financial assistance from the Australian Research Council and the Science Foundation for Physics within the University of Sydney. They would also like to thank Dr I. M. Bassett for helpful discussions.

References

[1] BASSETT, I. M., 1986, *Optica Acta*, **33,** 279.
[2] RICHARDS, B., and WOLF, E., 1959, *Proc. R. Soc.* A, **253,** 358.
[3] YOSHIDA, A., and ASAKURA, T., 1974, *Optik*, **40,** 321.
[4] YOSHIDA, A., and ASAKURA, T., 1975, *Optik*, **41,** 281.
[5] SHEPPARD, C. J. R., CHOUDHURY, A., and GANNOWAY, J. N., 1977, *IEE J. Microw., Optics Acoustics*, **1,** 129.
[6] SHEPPARD, C. J. R., 1978, *IEE J. Microw., Optics Acoustics*, **2,** 163.
[7] STAMNES, J. J., 1981, *Optics Commun.*, **37,** 311.
[8] LUNEBERG, R. K., 1966, *Mathematical Theory of Optics* (Berkeley, California: University of California Press).
[9] SHEPPARD, C. J. R., and GU, M., 1993, *J. mod. Optics*, **40,** 1631.
[10] INNES, D. J., and BLOOM, A. L., 1966, Spectra-Physics Laser Technical Bulletin No. 5.
[11] ABRAMOVITZ, M., and STEGUN, I., 1972, *Handbook of Mathematical Functions*, third edition (New York: Dover Publications).
[12] SHEPPARD, C. J. R., and MATTHEWS, H. J., 1987, *J. opt. Soc. Am.* A, **4,** 1354.
[13] STRATTON, J. A., 1941, *Electromagnetic Theory* (New York: McGraw-Hill).
[14] KANT, C., 1993, *J. mod. Optics*, **40,** 337.